Combination of X-ray tube and GMDH neural network as a nondestructive and potential technique for measuring characteristics of gas-oil–water three phase flows

Combination of X-ray tube and GMDH neural network as a nondestructive and potential technique for measuring characteristics of gas-oil-water three phase flows

Mohammadmehdi Roshani[1,2], Giang Phan[1], Gholam Hossein Roshani[3], Robert Hanus[4], Behrooz Nazemi[5], Enrico Corniani*[6,7] , Ehsan Nazemi[8]

[1] Institute of Fundamental and Applied Sciences, Duy Tan University, Ho Chi Minh city 700000, Vietnam.

[2] Faculty of Electrical – Electronic Engineering, Duy Tan University, Da Nang 550000, Vietnam.

[3] Electrical Engineering Department, Kermanshah University of Technology, Kermanshah, Iran.

[4] Rzeszów University of Technology, Faculty of Electrical and Computer Engineering, Rzeszów, Poland.

[5] Yazd University, Yazd, Iran.

[6] Division of Nuclear Physics, Advanced Institute of Materials Science, Ton Duc Thang University, Ho Chi Minh City, Vietnam (email: enrico.corniani@tdtu.edu.vn)

[7] Faculty of Applied Sciences, Ton Duc Thang University, Ho Chi Minh City, Vietnam.

[8] Imec-Vision Lab, Department of Physics, University of Antwerp, Antwerp, Belgium.

Abstract

In this investigation, a fan-beam photon attenuation based system, including one X-ray tube and two sodium iodide crystal detectors, combined with group method of data handling (GMDH) neural network is proposed to recognize type of flow regime and predict gas-oil-water volume fractions of a three phase flow. One GMDH neural network was considered for recognizing flow patterns and two GMDH networks were implemented to predict the volume fractions. The recorded photon energy spectra from the two sodium iodide detectors were defined as the inputs of the three GMDH neural networks. The type of flow pattern and volume fractions were the output obtained from the first and the other two GMDH neural networks, respectively. Through the application of the proposed methodology, all of the flow patterns were recognized correctly except one single case. The volume fraction was also predicted with RMS error of less than 3.1.

Keywords: GMDH neural networks; X-ray tube; Flow pattern; Volume fraction; Gas-oil-water; Three phase flow.

1. Introduction

Determining flow pattern and volume fraction of gas-oil-water three phase flow has been one of the major areas of interest in petroleum industry. Flow pattern has a direct influence on the separating process efficiency while the volume fraction of the each phase provides indication as to whether the drilling process should be continued or stopped [1]. Radiation Based Multi-Phase Flow Meter (RBMPFM) is one of the well-known types of MPFMs. Improving the efficiency and precision of the RBMPFMs and decreasing the problems of working with RBMPFMs are the main objectives of this manuscript.

Numerous studies have been devoted to investigating how to identify the flow regime in gas-oil-water three phase flows using photon radiation. In 2010, Salgado et al. proposed a radiation based method for recognizing flow regime of a 3 components (oil, water and gas) multiphase flow [2]. They used Monte Carlo N-Particle version X (MCNPX) code to model the proposed detection system as well as three flow patterns of homogeneous, stratified and annular with different volume fractions. Their proposed detection system included 2 radioisotope sources and 3 NaI detectors. They implemented four Artificial Neural Networks (ANNs) for determining the type of flow regimes and the volume fractions. The recorded photon spectrum in the detector was used as the input of first ANN and flow pattern type was obtained as the output. Other 3 ANNs with input same as the first ANN and volume fractions of 2 components as the outputs, were employed to estimate the volume fractions of each recognized flow regime. In 2012, Arvoh et al., used gamma measurement combined with multivariate calibration techniques to carry out some experiments at a large scale multiphase flow test facility with the aim of predicting volume fractions and recognizing flow patterns of slug (stratified-wavy, annular and dispersed) in a three phase flow [1]. Their system included one barium-133 source with an activity of 1.1×10^{8} Bq and a CnZnTd detector. In 2017, Roshani et al. proposed a method to recognize the flow patterns and predict volume fractions in a water-oil-gas multiphase system applying a dual energy fan-beam photon attenuation technique: the system included two radioisotopes of americium-241 and cesium-137 and two sodium iodide detectors, combined with ANN [3]; the recorded counts under the photo peaks of ^{241}Am and ^{137}Cs in two detectors was defined as the inputs for the ANN while the flow pattern's type was obtained as output. Using the above mentioned methodology, the authors succeeded to recognize all the flow patterns and also to determine volume fractions with mean absolute error of less than 5.68 %. Further researches in this field of study can be found in [4-20].

In the cited studies, different hardware structures and software have been used in three phase flow meters: various radioisotopes and detectors with different kinds of algorithms and artificial intelligences have been presented in these years but the problems of working with RBMPFMs are still remaining. Systems with radioisotope sources have specific photon energy and cannot be switched off like X-ray machines; therefore there is a continuous radiation emission with stochastic effects and this causes reluctance to use this kind of meters in various industries.

In this investigation, a fan-beam photon attenuation based system, including one X-ray tube and two sodium iodide crystal detectors, combined with GMDH neural network is proposed to recognize type of flow regime and predict water-oil-gas volume fractions of a three phase flow. In the present work one X-ray tube is utilized, while in all of the former studies one or some radioisotope sources were implemented in a radiation based three-phase flow meter to act as a photon emitter. It is important to highlight that X-ray tubes are of some advantages in comparison with radioisotope sources: for example the emitted photons have tunable energy, a much higher photon flux, an almost constant photon intensity over time and the possibility of turning on and off the photon emission etc. etc.

In this paper, different regimes of three phase flow and presented metering system using X-ray tube are modeled using MCNPX code. The procedure of modelling is given in the "System modelling" subsection of "Methodology" section. Determining the appropriate architectures of Group Method of Data Handling (GMDH) networks is given in the "GMDH" subsection. Obtained results are presented in the "Results" section and finally, investigation of presented system and comparison between this work and other former studies are given in the "Discussion and Analysis" section.

2. Methodology

2.1. System modelling

In the present work, Monte Carlo N-Particle code version X (MCNP-X) [21] has been used for physical modelling of the proposed measuring system. MCNPX code has the ability to consider three main photon interaction mechanisms with materials i.e photoelectron, Compton scattering, and pair production. This code has been widely implemented as a useful and powerful toolkit for modelling various radiation based systems.

The proposed detection system in this study is composed of one X-ray tube as the photon emitter and two 2.54 mm x 2.54 mm sodium iodide crystal as the detectors. A Pyrex-glass pipe was also considered such that the various flow patterns and volume fractions are easily modelled inside it.

To model the sodium iodide detector, a homogeneous cylinder with diameter and thickness of 2.54 mm was considered. The first detector was positioned in front of the X-ray tube at a distance of 20 cm from that. The second one was positioned at the same distance from the X-ray tube but with an orientation of 15^{o} respect to the connecting line of the tube and the first detector. Using tally type 8 (pulse-height tally), the energy spectra of transmitted photons were recorded in both detectors. To account for the photon spectrum broadening the FT8 Gaussian Energy Broadening (GEB) card in the MCNPX code's input file was also utilized. The required inputs for the mentioned card were calculated in a previous work [22] for a sodium iodide crystal detector similar to the one used in this investigation (from point of view of dimensions as well as material). Tally energy card (E8) was defined in a way to separate the output into 100 bins (each bin is a fixed energy slot of 2 keV) with the aim of extracting transmitted photon's energy spectrum. The simulated system and detectors' position are schematically shown in Fig. 1.

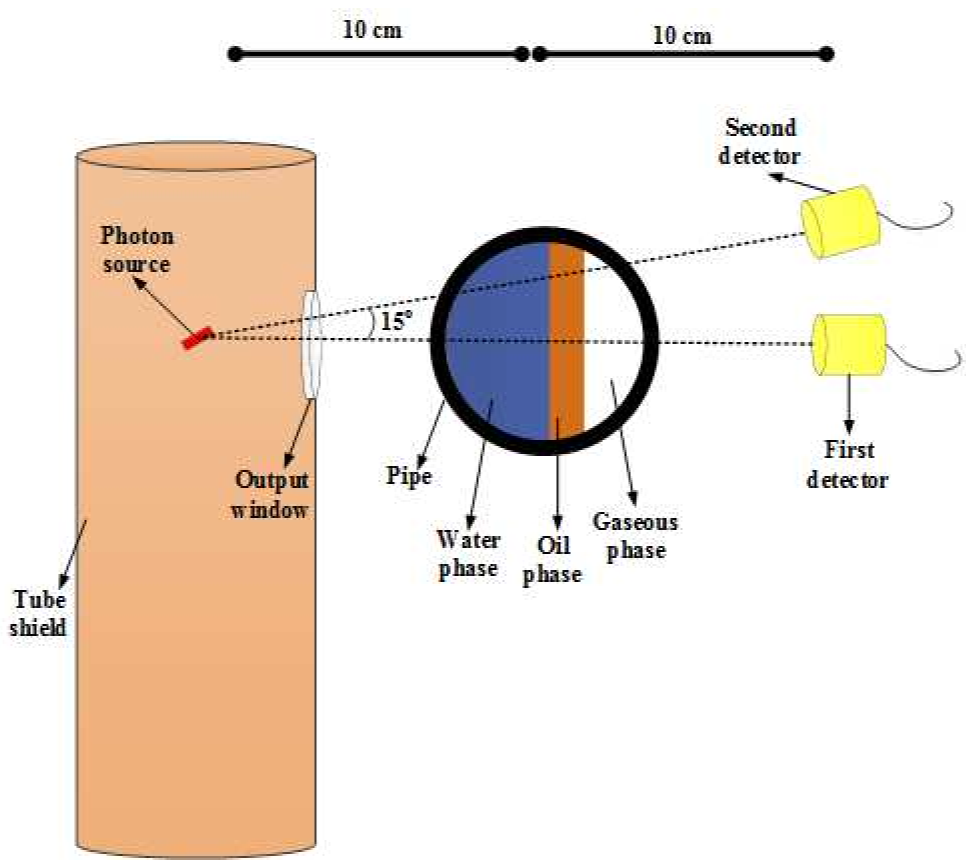

Fig. 1- The simulated detection system and locations of two detectors.

In this investigation a conventional industrial X-ray tube was implemented as the X-ray radiation generator. Because photon tracking in MCNPX code takes less time compared to electron tracking, a photon source embedded in the shield of an X-ray tube was considered in this study instead of a cathode that emits electrons. TASMIC package presented by Hernandez et. al [23] was exploited for modelling the required photon source. A rectangular planner with width and length of 1 mm x 10 mm and an inclination of 12^o with respect to the connected line of source and detector was defined as the photon source, these dimensions were chosen in accordance with reference [23]. The MCNPX modelled energy spectrum of the photon source corresponded to an X-ray tube with 200 kilovoltage peak (kV_p) filtered by a 1 mm aluminium sheet. It is worth mentioning that filtering and removing low energy photons leads to a reduction in photon scattering. The photon source was placed within a cylinder that acts like an X-ray tube shield.

As schematically shown in Fig. 2, three basic flow patterns of stratified, annular, and homogenous with different volume fractions were modelled in this investigation. Oil, gas, and water phases were substituted with gasoil, air, and water with densities of 0.826, 0.00125, and 1 g/cm^3, respectively. In the case of stratified and annular flow patterns, different combinations of volume fractions were obtained by altering the portion of each phase. For homogeneous flow pattern, just one fluid (mixture of gasoil, air, and water) was considered inside the pipe. Different volume fractions were achieved by altering density of the mixture as well as the mass fraction of each component. Although the modelled homogenous flow pattern in this investigation is an ideal case and is slightly different from the real homogenous pattern that occurs in multiphase flows, this system is easy and suitable for simulation because of its symmetry; other researchers adopted this model to simulate the homogenous regime [2, 10, 24]. Different volume fractions in the range of 10-80 % with steps of 10% were replicated for all of the three flow patterns. Thirty-six modelled combinations of gas, oil, and water volume fractions for each flow pattern are shown in Fig. 3 which presents a graphical representation called ternary. This Plot is a barycentric plot on three variables which sum is a constant. In total 108 simulations were carried out in this study.

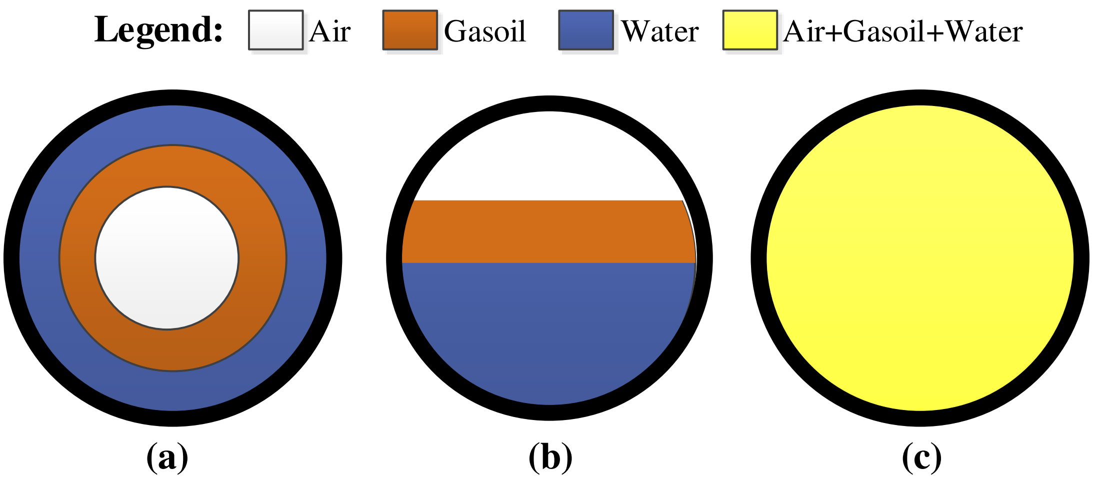

Fig. 2- Modelled flow patterns: a) annular b) stratified c) homogenous.

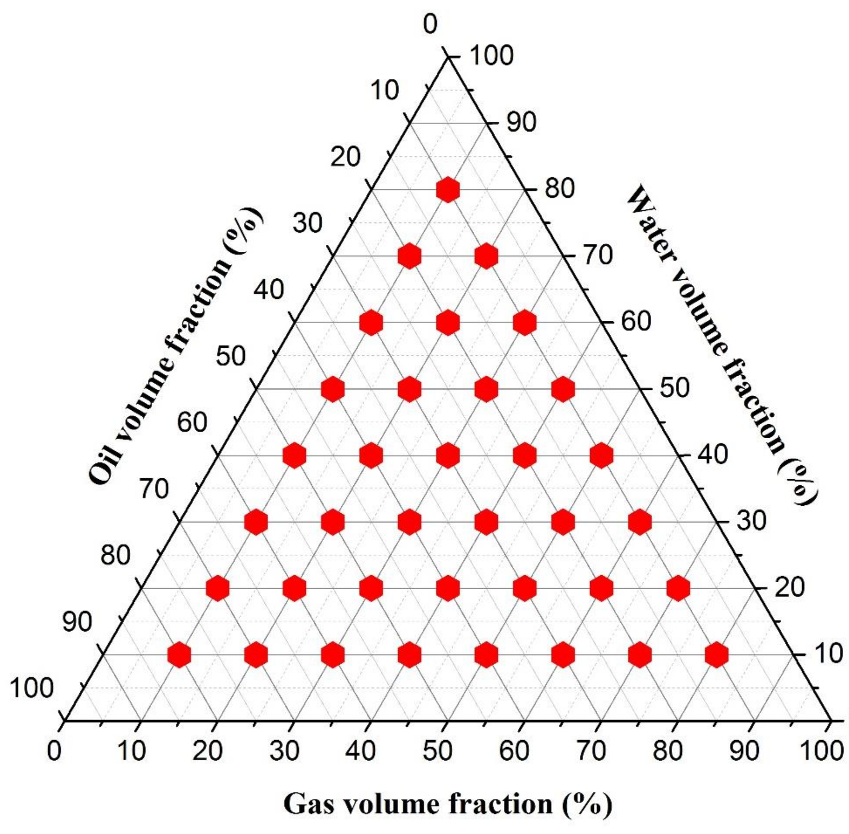

Fig. 3- Different modelled combinations of gas, oil, and water volume fractions.

2.2. GMDH

Group Method of Data Handling (GMDH) is a kind of Artificial Neural Networks (ANN) which has been presented by Ivakhnenko [25]. Nowadays, different kinds of Artificial Neural Networks are implemented in order to solve various engineering problems [26-27]. The GMDH ANN which was used in this study is a strong tool in prediction, data mining, optimization and pattern recognition problems. The network structure consists of several layers, several neurons in each layer and inputs that are selected in a self-organized manner. The input-output relation in GMDH method is described by the Kolmogorov-Gabor polynomial as follow:

$$y = a_0 + \sum_{i=1}^{m} a_i x_i + \sum_{i=1}^{m} \sum_{j=1}^{m} a_{ij} x_i x_j + \sum_{i=1}^{m} \sum_{j=1}^{m} \sum_{k=1}^{m} a_{ijk} x_i x_j x_k + \cdots \qquad (1)$$

In Kolmogorov-Gabor polynomial; y, x ($x_1, x_2, \ldots, x_m$) and a ($a_1, a_2, \ldots, a_m$) are network output, input vector and coefficient vector, respectively. GMDH approach is very strong tool for modelling but only one output is allowed using it. Mathematical structure of GMDH approach and usage of Kolmogorov-Gabor polynomial are reasons of this fact.

In the training procedure, new variables are generated from old variables. In this study, the output spectra of the two detectors were divided to 200 energy bins and these energy bins were fed to the GMDH neural networks as 200 independent variables. The system was modelled by pluggin-in in equation 2 every pair of two independent variables.

$$V = c_1 + c_2 x_i + c_3 x_j + c_4 {x_i}^2 + c_5 {x_j}^2 + c_6 x_i x_j \qquad (2)$$

The differences between real output and predicted one for all input variables was minimized by applying the regression techniques for computing the coefficients c_i in (2). The combinations with higher error rates were removed and the outputs of other combinations were considered as new independent variables. This procedure was continued until one output with minimum error rate was found. Obviously the network structure has direct influence on the results and using this presented self-organization manner the appropriate architecture could be obtained. The low error in the training procedure shows the precision of the model but in order to check the validity of the model also a low yesy data error is required. To test the presented neural networks, the designed networks were evaluated using testing data. In this study about 70% (76 samples) and about 30% (32 samples) of data were used to train and test the neural networks, respectively. The low error of the obtained model during the testing procedure shows the goodness of the model and proves its efficiency.

The above described GMDH was then used to recognize the regime of three phase flow and measure the volume fractions of each component implementing X-ray tube as radiation source. 200 features were extracted from output spectra of both sodium iodide crystal detectors. The spectra were divided to 200 bins, from 0 to 200 keV with the 2 keV steps. These features were named Bin1 to Bin100 for first detector and Bin101 to Bin200 for second detector. The extracted features were considered as the inputs of GMDH neural networks. Three different networks with the aim of recognizing the flow pattern, predict the oil fraction and predict the gas fraction were designed. The architectures of the three presented GMDH networks were illustrated in Fig. 4. Each neuron was plotted by a circle and connection of neurons was illustrated by lines.

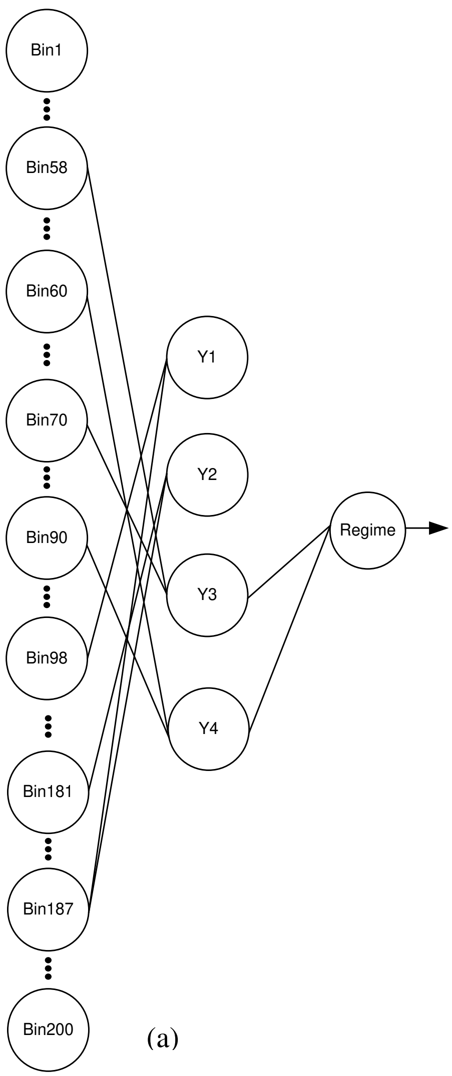

(a)

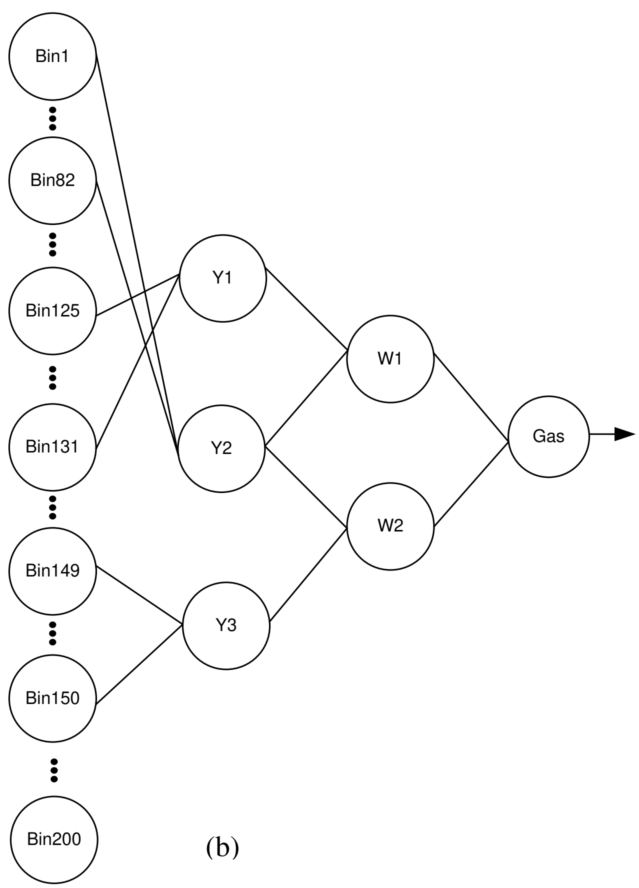

(b)

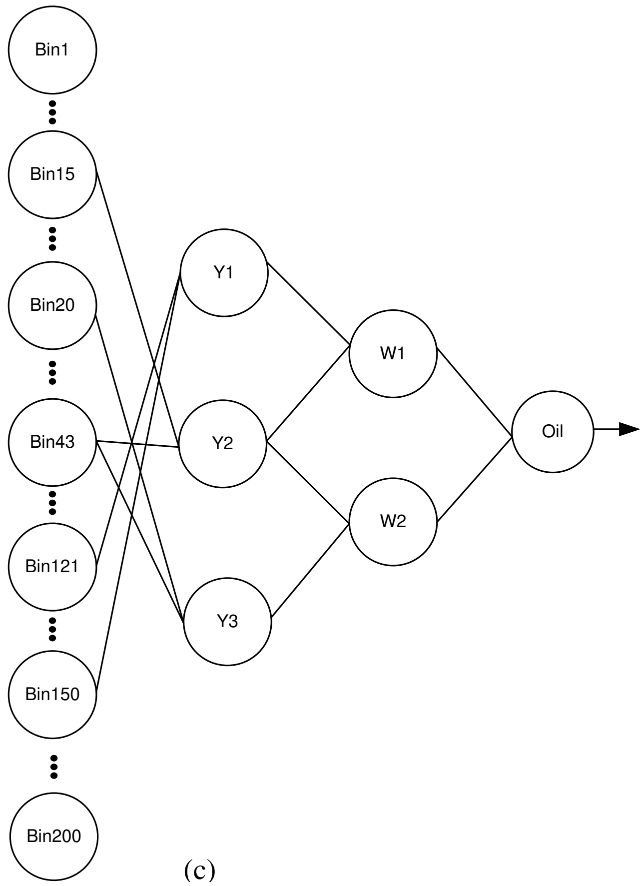

(c)

Fig. 4- The designed GMDH neural network's architecture for a) Flow regime identification b) Gas fraction measurement c) Oil fraction measurement

The output polynomials of each hidden layer are tabulated in Table 1. This table indicates the output equation and coefficients of each neuron.

Table 1- The output polynomials of each hidden layer for three presented GMDH models.

GMDH neural network for flow regime identification	
The output equation of each neuron	The coefficients of each equation
$Y_1=C_1+C_2.Bin_{98}+C_3.Bin_{187}+C_4.Bin_{98}^2+C_5Bin_{187}^2+C_6.Bin_{98}.Bin_{187}$	C=[2.35,-273.48,51.62,-5493.86,-328.46,2849.63]
$Y_2=C_1+C_2.Bin_{181}+C_3.Bin_{187}+C_4.Bin_{181}^2+C_5Bin_{187}^2+C_6.Bin_{181}.Bin_{187}$	C=[5.99,-7.89,-60.92,1411.07,3957.90,-4555.22]
$Y_3=C_1+C_2.Bin_{58}+C_3.Bin_{70}+C_4.Bin_{58}^2+C_5Bin_{70}^2+C_6.Bin_{58}.Bin_{70}$	C=[6.28,50.09,-98.95,179.13,556.37,-622.66]

$Y_4=C_1+C_2.Bin_{60}+C_3.Bin_{90}+C_4.Bin_{60}^2+C_5Bin_{90}^2+C_6.Bin_{60}.Bin_{90}$	C=[4.00,-51.43,291.91,138.65,3699.95,-1447.13]
$Regime=C_1+C_2.Y_3+C_3.Y_4+C_4.Y_3^2+C_5Y_4^2+C_6.Y_3.Y_4$	C=[-0.24,0.20,0.98,0.21,0.02,-0.28]
GMDH neural network for gas fraction measurement	
The output equation of each neuron	The coefficients of each equation
$Y_1=C_1+C_2.Bin_{125}+C_3.Bin_{131}+C_4.Bin_{125}^2+C_5Bin_{131}^2+C_6.Bin_{125}.Bin_{131}$	C=[-80.68,169.00,-47.28,-934.88,-391.76,1203.24]
$Y_2=C_1+C_2.Bin_1+C_3.Bin_{82}+C_4.Bin_1^2+C_5Bin_{82}^2+C_6.Bin_1.Bin_{82}$	C=[-73.14,131.30,428.07,-1241.66,-905.56,2190.89]
$Y_3=C_1+C_2.Bin_{149}+C_3.Bin_{150}+C_4.Bin_{149}^2+C_5Bin_{150}^2+C_6.Bin_{149}.Bin_{150}$	C=[-94.23,451.00,-231.96,5358.13,5983.81,-11408.36]
$W_1=C_1+C_2.Y_1+C_3.Y_2+C_4.Y_1^2+C_5Y_2^2+C_6.Y_1.Y_2$	C=[-3.00,0.34,0.78,0.02,0.02,-0.05]
$W_2=C_1+C_2.Y_2+C_3.Y_3+C_4.Y_2^2+C_5Y_3^2+C_6.Y_2.Y_3$	C=[-4.52,0.59,0.63,0.01,0.00,-0.02]
$Gas=C_1+C_2.W_1+C_3.W_2+C_4.W_1^2+C_5W_2^2+C_6.W_1.W_2$	C=[-0.98,0.41,0.67,-0.02,-0.04,0.07]
GMDH neural network for oil fraction measurement	
The output equation of each neuron	The coefficients of each equation
$Y_1=C_1+C_2.Bin_{121}+C_3.Bin_{150}+C_4.Bin_{121}^2+C_5Bin_{150}^2+C_6.Bin_{121}.Bin_{150}$	C=[78.91,802.53,-1614.06,-5.77,1429.72,-725.93]
$Y_2=C_1+C_2.Bin_{15}+C_3.Bin_{43}+C_4.Bin_{15}^2+C_5Bin_{43}^2+C_6.Bin_{15}.Bin_{43}$	C=[221.38,577.31,-929.78,183.03,793.21,-835.49]
$Y_3=C_1+C_2.Bin_{20}+C_3.Bin_{43}+C_4.Bin_{20}^2+C_5Bin_{43}^2+C_6.Bin_{20}.Bin_{43}$	C=[166.31,775.97,-1434.51,411.87,2041.99,-1898.94]
$W_1=C_1+C_2.Y_1+C_3.Y_2+C_4.Y_1^2+C_5Y_2^2+C_6.Y_1.Y_2$	C=[-2.31,0.70,0.42,-0.01,-0.00,0.02]
$W_2=C_1+C_2.Y_2+C_3.Y_3+C_4.Y_2^2+C_5Y_3^2+C_6.Y_2.Y_3$	C=[-1.72,0.43,0.71,-0.04,-0.05,0.09]
$Oil=C_1+C_2.W_1+C_3.W_2+C_4.W_1^2+C_5W_2^2+C_6.W_1.W_2$	C=[0.20,0.98,0.01,-0.02,-0.02,0.05]

The process flow of this study is shown in Fig. 5.

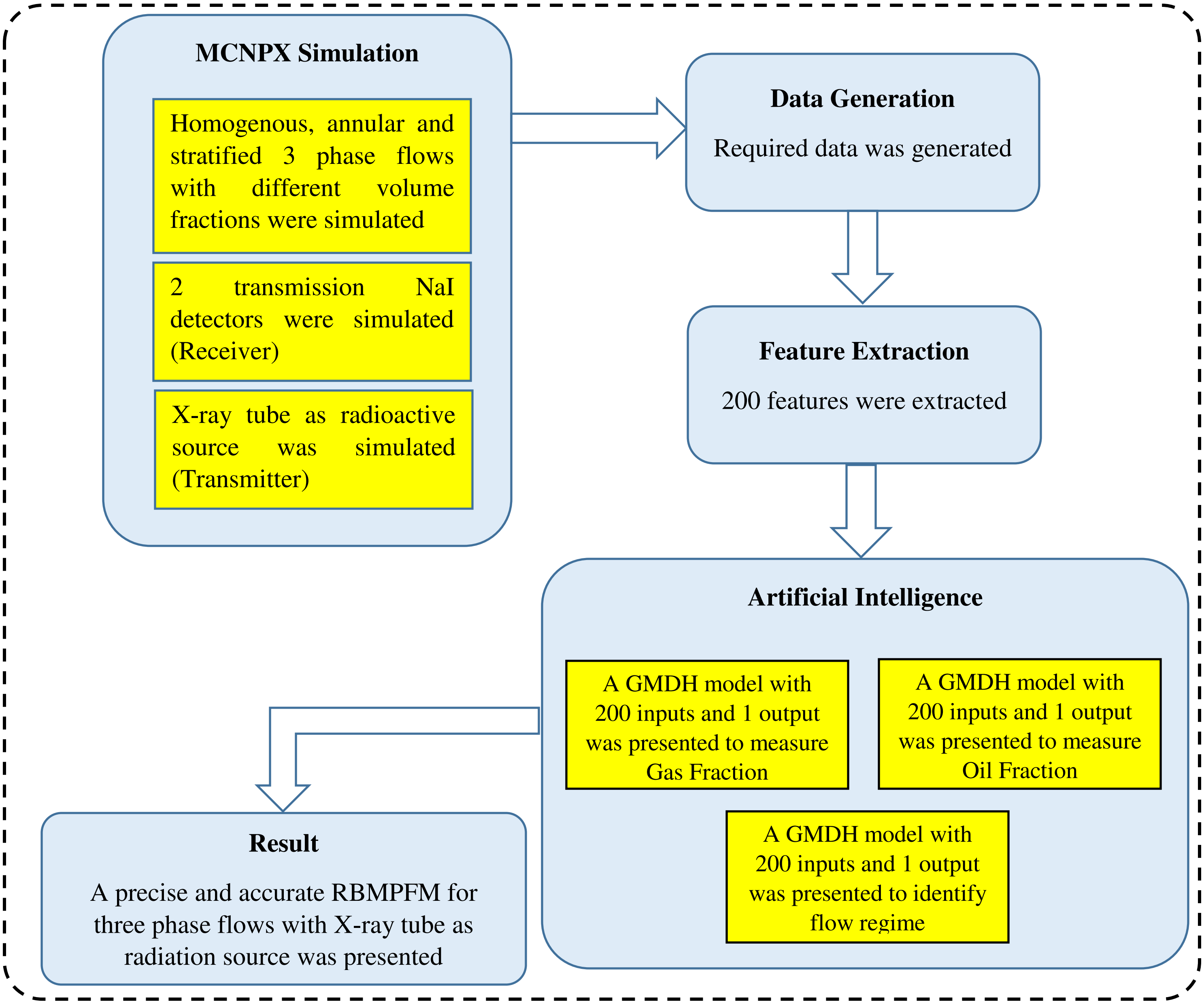

Fig. 5- The process of presented study

It was mentioned previously that the Monte Carlo code MCNPX code was used to simulate the metering system and MATLAB software was used to implement the mathematical equations of GMDH models.

3. Results

Figure 6 reports an example of recorded spectra from both detectors in a simulated anular regime with different volume fractions of oil-water-gas. Comparing the detectors, it can be seen that the spectrum intensity from the first detector as well as the discrepancy between spectra related to different volume fractions is higher than in the second one. Comparing Fig. 6(a) with Fig. 6(b) and with Fig. 6(c), it can be observed that discrepancy between spectra when gas volume fraction is kept fixed and liquid phases (oil or water) volume fractions are changed (Fig. 6(a)), is less than when liquid phases volume fractions are kept constant and gas volume fraction is changed (Fig. 6(b) and Fig. 6(c)). In other words, the sensitivity of this system in distinguishing between gas phase and liquid phases is much higher than recognizing oil from water phase. The reason resides in the fact that the photon mass attenuation coefficients of oil and water phases are close to each other, while both values are are much higher compared to the coefficient for the gas phase.

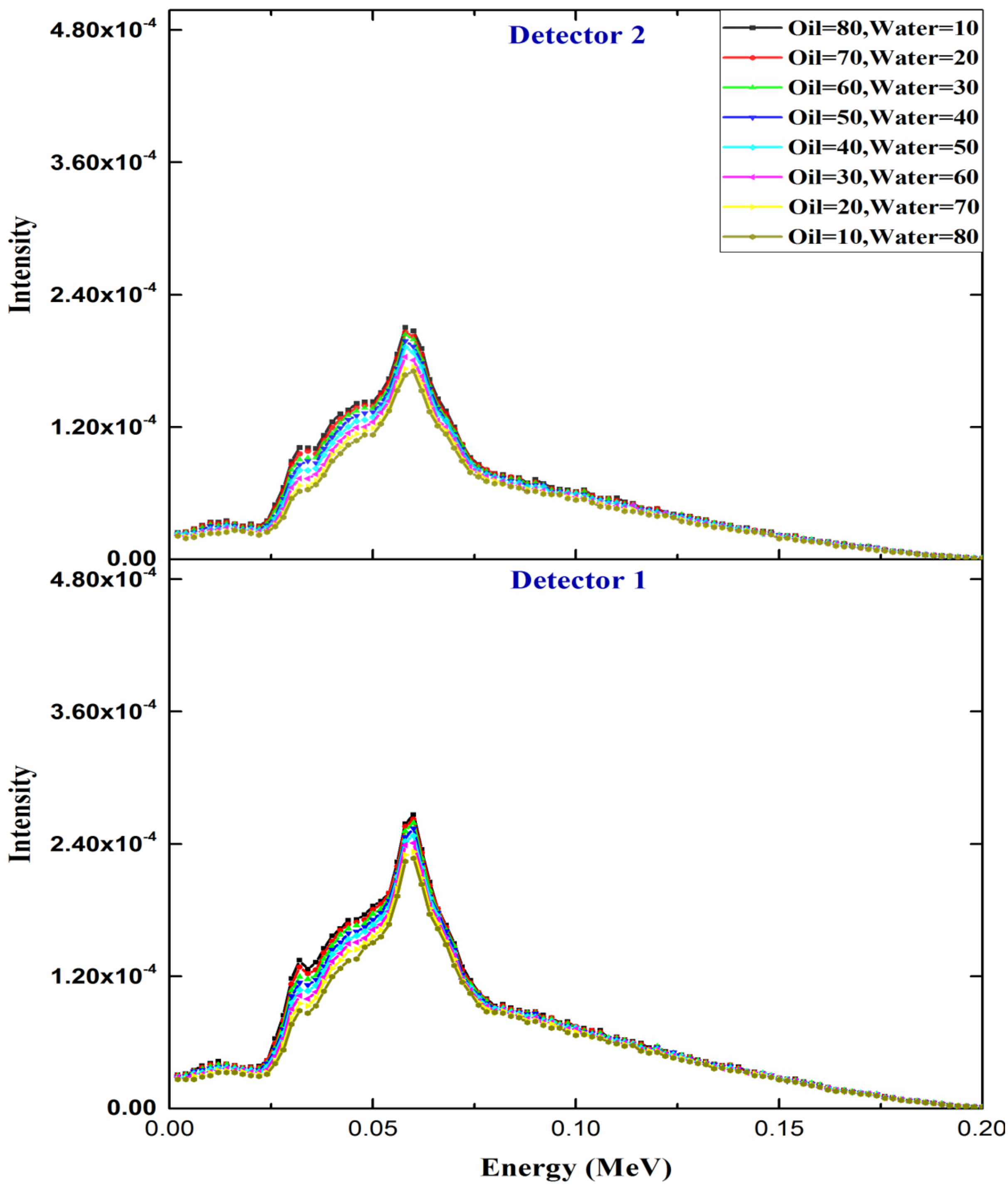

Detector 2
Detector 1
Oil=80,Water=10
Oil=70,Water=20
Oil=60,Water=30
Oil=50,Water=40
Oil=40,Water=50
Oil=30,Water=60
Oil=20,Water=70
Oil=10,Water=80
Intensity
4.80x10^-4
3.60x10^-4
2.40x10^-4
1.20x10^-4
0.00
0.00
0.05
0.10
0.15
0.20
Energy (MeV)

(a)

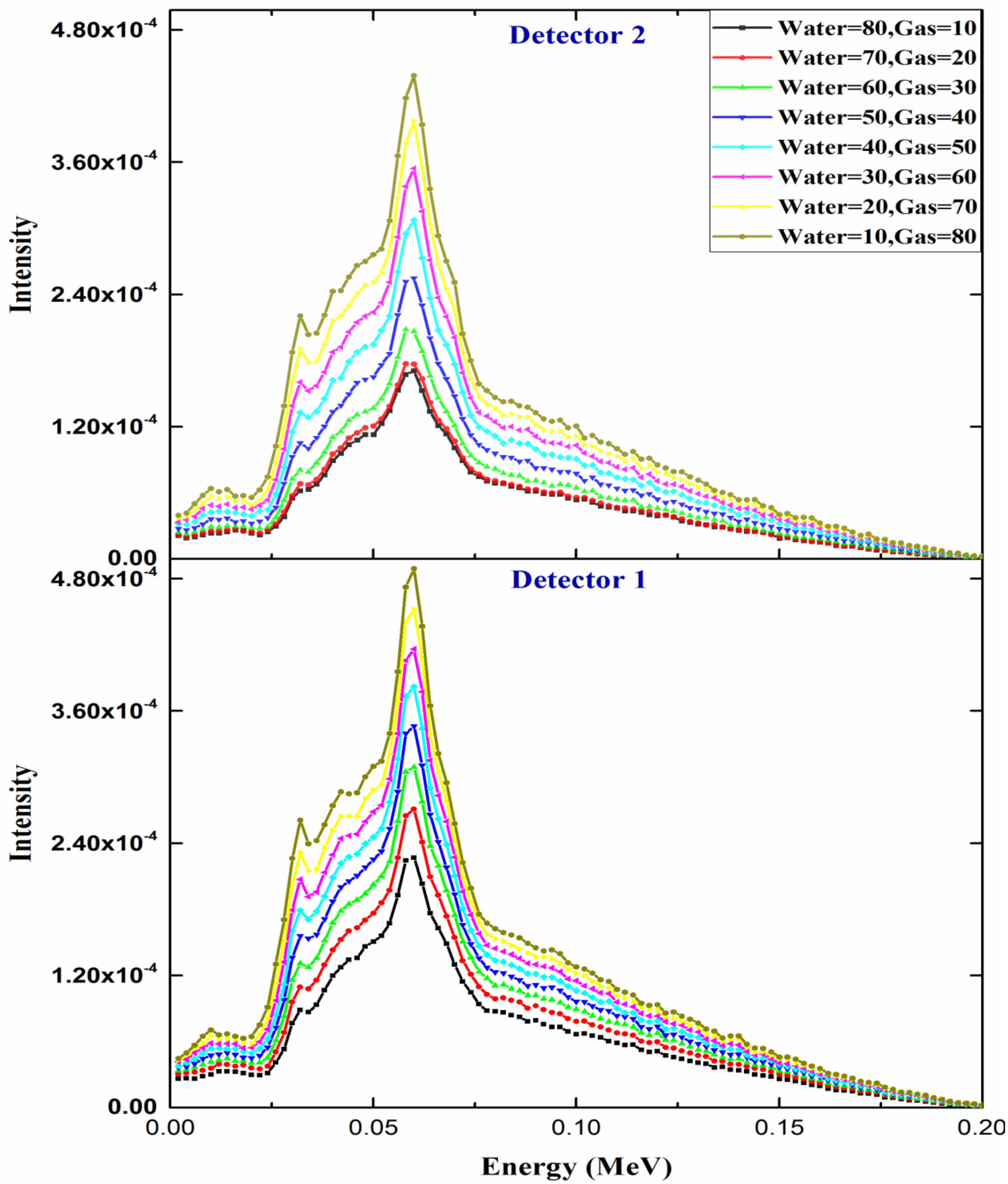
Detector 2
Detector 1
Water=80,Gas=10
Water=70,Gas=20
Water=60,Gas=30
Water=50,Gas=40
Water=40,Gas=50
Water=30,Gas=60
Water=20,Gas=70
Water=10,Gas=80
Intensity
Energy (MeV)
4.80x10^-4
3.60x10^-4
2.40x10^-4
1.20x10^-4
0.00
0.00
0.05
0.10
0.15
0.20

(b)

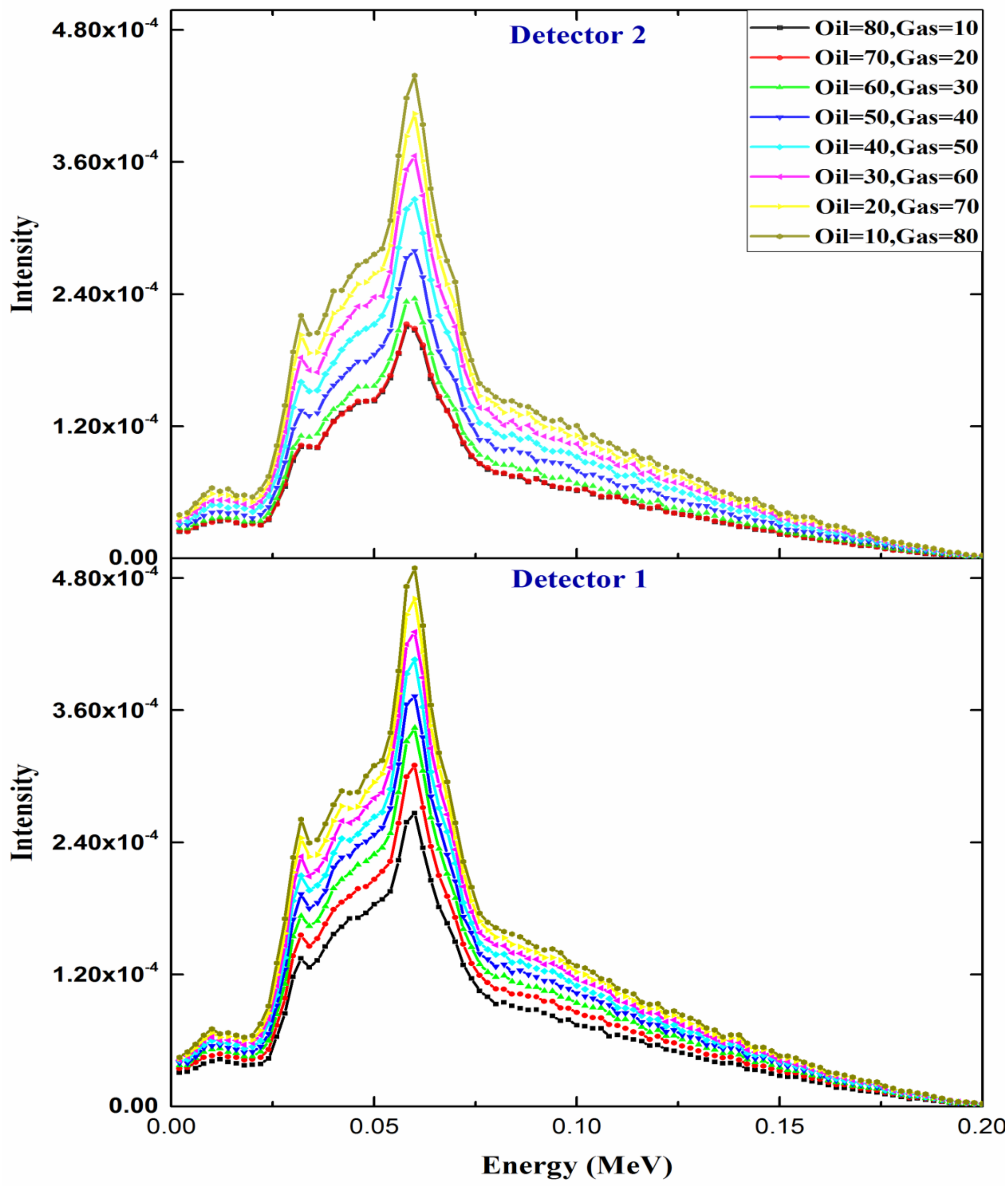

(c)

Fig. 6- Recorded photon energy spectra in both detectors for annular regime: a) Gas volume fraction is 10 %, water and oil volume fractions are in the range of 10-80 % b) Oil volume fraction is 10 %, water and gas volume fractions are in the range of 10-80 % c) Water volume fraction is 10 %, gas and oil volume fractions are in the range of 10-80 %.

The difference between actual and predicted data as well as regression diagrams for training and testing data sets is shown in Figs. 7 and 8 to illustrate the performance of the implemented networks. Fig. 9 resumes the performance of the presented network in identifying the flow regime. The targets of GMDH model were 1 for annular regime, 2 for homogenous regime and 3 for stratified regime but it is clear that there is a small mismatch between outputs and targets. Hence at the end of GMDH model network outputs of less than 1.5, between 1.5 and 2.5 and higher than 2.5 were defined to correspond respectively to a flow regime of annular, homogenous and stratified. Fig. 9 illustrates that all of the regimes have been determined correctly except one. In fact only one mistake occurred in 108 cases which shows the precision of presented network for flow regime identification. To evaluate the proposed networks, Root Mean Square Error (RMSE), Mean Absolute Error (MAE) and Mean Absolute Percentage Error (MAPE) were obtained according to equations 3, 4 and 5. RMSE and MAE results have been reported in Table 2.

$$RMSE = \left[\frac{\sum_{j=1}^{N}(X_j(actual)-X_j(predicted))^2}{N}\right]^{0.5} \quad (3)$$

$$MAE = \frac{1}{N}\sum_{j=1}^{N}\left|X_j(actual)-X_j(\mathrm{Pr}edicted)\right| \quad (4)$$

$$MAPE = \frac{1}{N}\sum_{j=1}^{N}\left|\frac{X_j\left(actual\right)-X_j\left(predicted\right)}{X_j\left(actual\right)}\right| \quad (5)$$

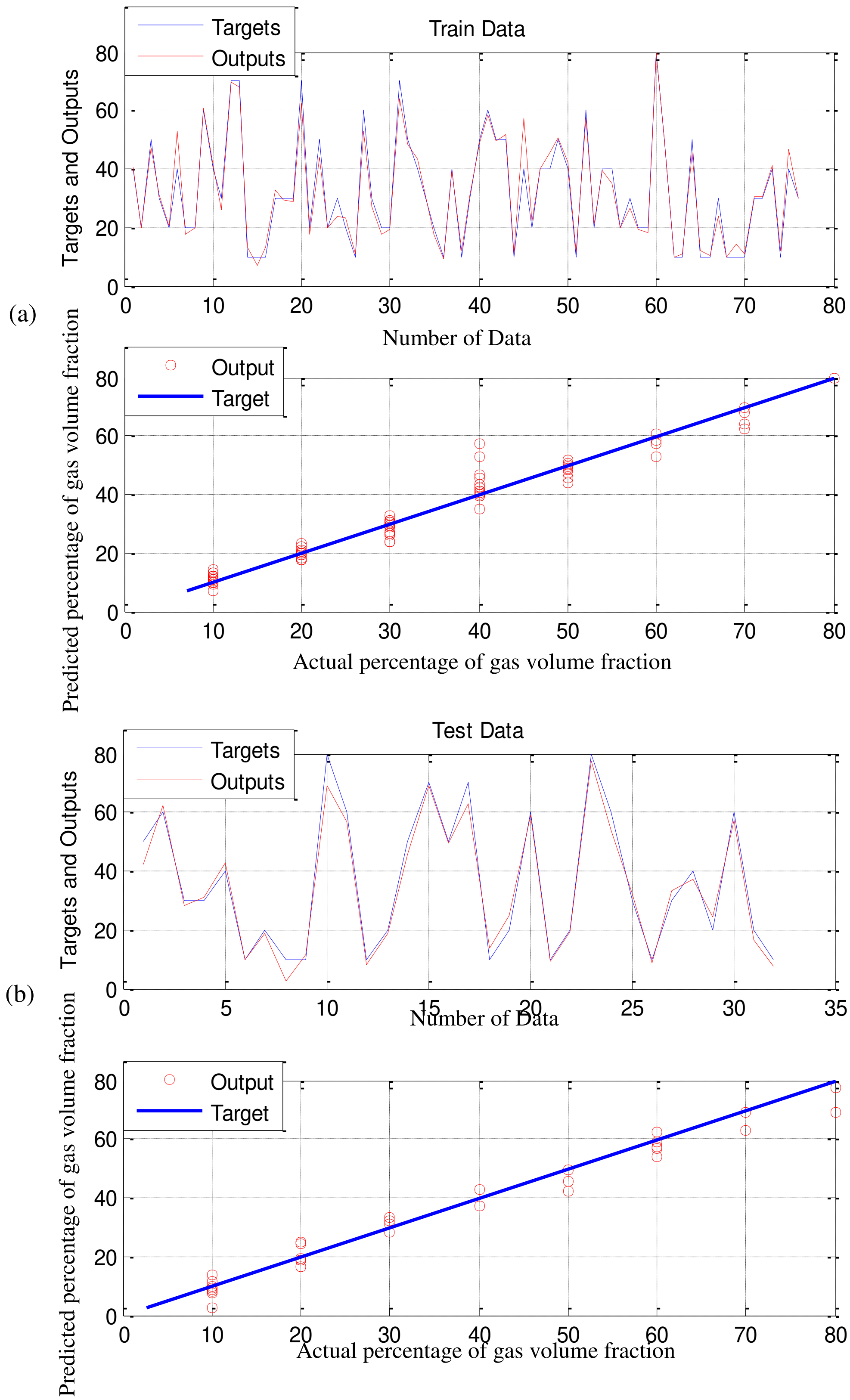

Fig. 7- Performance of GMDH neural network for measuring the gas fraction: a) training, b) testing

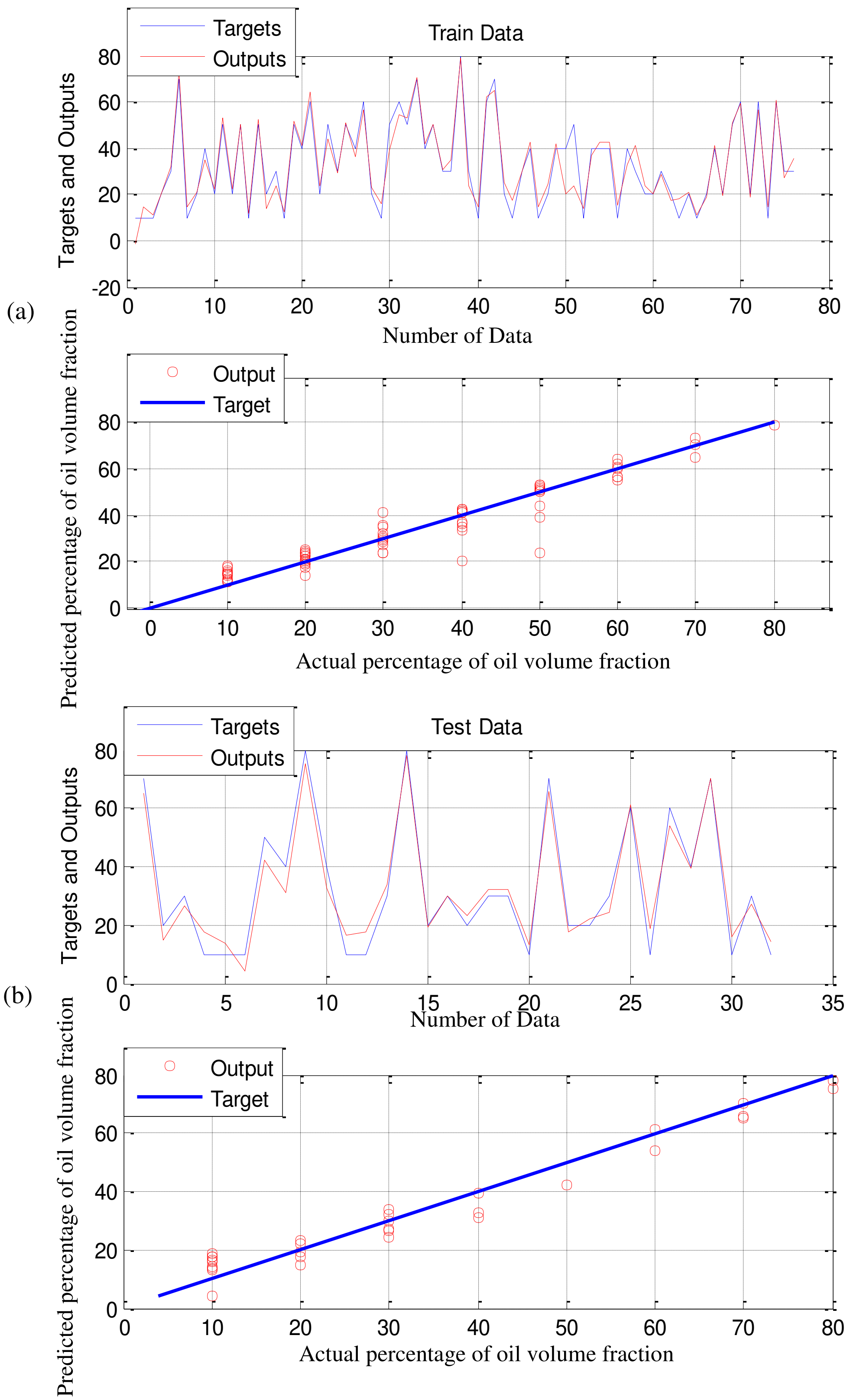

Fig. 8- Performance of GMDH neural network for measuring the oil fraction: a) training, b) testing

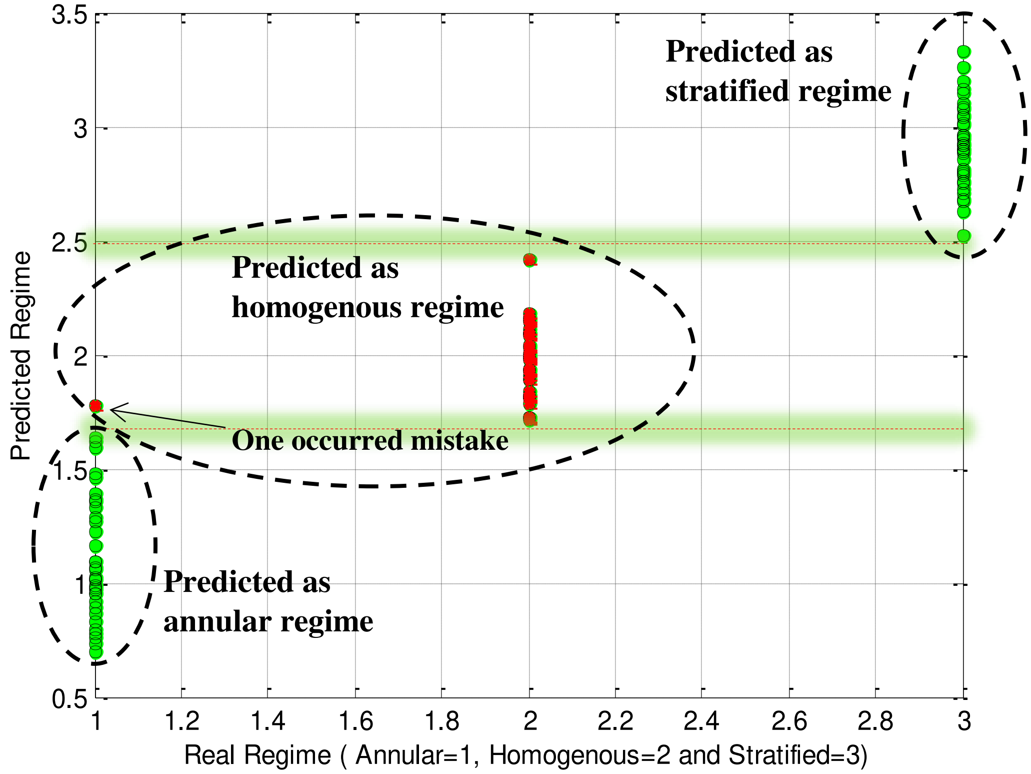

Fig. 9- Performance of GMDH neural network for recognizing flow pattern in both training and testing sets

Table 2- Obtained errors of GMDH networks

Output	RMSE Train	RMSE Test	MAE Train	MAE Test	MAPE Train	MAPE Test
Gas Fraction	3.76	3.88	2.57	3.00	0.09	0.11
oil Fraction	5.39	4.89	3.92	4.22	0.19	0.23

4. Discussion and Analysis

X-ray technology is now used in a wide variety of applications and settings. In this study, it was tried to use X-ray technology in another way. Regime identification and volume fraction measurement were obtained using combination of X-ray attenuation technique and Artificial Intelligence. In fact, the changes in volume fractions and flow patterns were related to output spectrum of detectors using X-ray attenuation technique. This relation was obtained using AI and consequently a novel measuring system was presented.

The following Table 3 presents a comparison between the current investigation and other former studies.

Table 3- Comparison between current investigation and former studies

Reference	Flow regime	Number of Detectors	Feature Extraction	Source	Regime Detection	Volume Fraction Measurement	Type of Network	MRE % Train	MAE Train	RMSE Train	MRE % Test	MAE Test	RMSE Test
[2]	Three Phase (Annular, Stratified and Homogeneous)	2	Whole Spectrum as Input	Cs-137 & Am-241	✓	✓	MLP	3.5	-	-	3.5	-	-
[28]	Three Phase (Stratified)	1	Full energy Peaks	Cs-137 & Eu-152	-	✓	Jaya-ANFIS	0.40	-	0.39	1.31	-	0.56
[29]	Three Phase (Annular)	1	Full Energy Peaks	Cs-137& Eu-152	-	✓	ANFIS	0.34	-	-	2.73	-	-
[30]	Three Phase (Annular)	1	Full Energy Peaks	(Am-241&Cs-137), (Co-60&Cs-137), (Ba-133&Cs-137), (Ba-133&Am-241), (Am-241&Co-60) and (Ba-133&Co-60)	-	✓	Jaya-MLP	0.47	-	0.00	0.97	-	0.23
[31]	Three Phase (stratified)	1	Whole Spectrum as Input	Cs-137	-	✓	MLP	6.47	-	1.6	6.47	-	1.6
[32]	Three Phase (stratified)	1	Whole Spectrum as Input	Co-60	-	✓	MLP	4.64	-	1.49	4.64	-	1.49
[33]	Three Phase (stratified)	1	Whole Spectrum as Input	Cs-137	-	✓	MLP	7.08	-	2.48	7.08	-	2.48
This study	Three Phase (Annular, Stratified and	2	Whole Spectrum as Input	X-Ray Tube	✓	✓	GMDH	-	3.92	5.39	-	4.22	4.89

	Homogeneous)												

As it appears from Table 3, various radioisotope sources in the form of single or dual energy emitters such as Cs-137, Co-60, (Am-241&Cs-137), (Co-60&Cs-137), (Ba-133&Cs-137), (Ba-133&Am-241), (Am-241&Co-60), (Ba-133&Co-60) and (Cs-137 & Eu-152) have been used so far in three phase flow measuring. In the presented system, radioisotope sources were replaced by an X-ray tube which has several advantages in comparison with radioisotope sources. Radioisotope sources cannot be switched off like X-ray machines; therefore there is continuous radiation dose in specific area. Consequently, there is reluctance to use this kind of meters in various industries. Tunable energy for emitted photons, much higher photon flux, constant photon intensity over time and etc are some of the other benefits of an X-ray tube. Combination of X-ray tube, GMDH network and two scintillation detectors is a powerful tool in three phase flows which helps in determining the flow regime and metering the volume fractions simultaneously. Generally speaking the presented system is robust on recognition and prediction because the applied artificial intelligence, with low testing set error, offers the possibility of interpolation. The proposed method is stable also because the source, detectors and computational process are stable. Although the precision of presented system is high it could be improved using different techniques: optimizing the voltage of X-ray tube, optimizing the applied artificial intelligence and usage of optimized feature extraction method can improve the precision of this presented system. These topics are the basis for further researches.

5. Conclusions

In this paper, applicability of X-ray tube combined with GMDH neural network as a strong metering device in three phase flows, was investigated. GMDH was implemented to recognize the regime of three phase flow and measure the volume fraction of each component using X-ray tube as radiation source. Two transmitted detectors, a pipe, three different regimes with various volume fractions of oil, water, and gas, X-ray tube and other details were simulated using MCNPX code. The networks were simulated using MATLAB software. 200 features were extracted from output spectra of both sodium iodide crystal detectors. The spectra were divided to 200 bins which were regarded as the GMDH neural network's inputs. Three different networks were designed with the aim of recognizing the flow pattern, predicting the oil fraction and predicting the gas fraction. Only one mistake occurred in 108 tests which indicates the precision of the proposed network for flow regime identification. The maximum MAE of this network for predicting the volume fractions was 4.22 which shows the precision of presented system. The system with radioisotope sources cannot be switched off like a system with X-ray tube; therefore there is continuous radiation emission and this creates reluctance in various industries that limits its use. Hence by replacing the radioisotope source with an X-ray tube some safety and regulatory concerns are removed and this should benefit the acceptance of these multiphase flows meters. Tunable energy for emitted photons, much higher photon flux, constant photon intensity over time and etc. are some of other benefits of the presented system.

Appendix A: Simulated and Predicted Data

The comparison of simulated and estimated values of gas and oil volume fraction percentages for testing data samples were tabulated in Table A1.

Table A1 – Comparison of simulated and predicted values of gas and oil volume fraction percentages for testing data samples

Data number	Simulated gas volume fraction	Predicted gas volume fraction percentages using GMDH	Absolute error between simulated and predicted gas volume fractions	Simulated oil volume fraction	Predicted oil volume fraction percentages using GMDH	Absolute error between simulated and predicted oil volume fractions
1	50	41.97	8.02	70	65.44	4.55
2	60	62.21	2.21	20	14.71	5.28
3	30	28.27	1.72	30	26.83	3.16
4	30	30.94	0.94	10	17.73	7.73
5	40	42.89	2.89	10	13.90	3.90
6	10	10.04	0.04	10	3.94	6.05
7	20	18.67	1.32	50	42.39	7.60
8	10	2.73	7.26	40	31.06	8.93
9	10	11.20	1.20	80	75.27	4.72
10	80	69.09	10.90	40	32.70	7.29
11	60	56.80	3.19	10	16.38	6.38
12	10	8.10	1.89	10	17.50	7.50
13	20	19.01	0.98	30	33.57	3.57
14	50	45.61	4.38	80	77.88	2.11
15	70	68.99	1.00	20	19.14	0.85
16	50	49.70	0.29	30	29.99	0.00
17	70	62.86	7.13	20	23.35	3.35

18	10	13.45	3.45	30	31.95	1.95
19	20	24.74	4.74	30	32.28	2.28
20	60	58.90	1.09	10	13.14	3.14
21	10	9.09	0.90	70	65.72	4.27
22	20	19.43	0.56	20	17.78	2.21
23	80	77.26	2.73	20	22.05	2.05
24	60	54.23	5.76	30	24.31	5.68
25	30	31.99	1.99	60	61.53	1.53
26	10	8.63	1.36	10	18.72	8.72
27	30	33.11	3.11	60	53.98	6.01
28	40	37.47	2.52	40	39.30	0.69
29	20	24.07	4.07	70	70.41	0.41
30	60	57.08	2.91	10	15.96	5.96
31	20	16.74	3.25	30	27.31	2.68
32	10	7.67	2.32	10	14.34	4.34

References

[1] B. Kaku Arvoh, R. Hoffmann, M. Halstensen, Estimation of volume fractions and flow regime identification in multiphase flow based on gamma measurements and multivariate calibration, Flow Measurement and Instrumentation, 23, 1 (2012), 56-65.

[2] C. M. Salgado, C. M. N. A. Pereira, R. Schirru, L. E.B. Brandao, Flow regime identification and volume fraction prediction in multiphase flows by means of gamma-ray attenuation and artificial neural networks, Progress in Nuclear Energy, 52 (2010), 555-562.

[3] G.H. Roshani, E, Nazemi and M. M. Roshani, Intelligent recognition of gas-oil-water three-phase flow regime and determination of volume fraction using radial basis function. Flow Measurement and Instrumentation, 54 (2017), pp.39-45.

[4] G. H. Roshani, S. Roshani, E. Nazemi and S. Roshani, Online measuring density of oil products in annular regime of gas-liquid two phase flows, Measurement, 129 (2018), 296–301.

[5] C. Sætre, S. Tjugum, G. A. Johansen, Tomographic segmentation in multiphase flow measurement, Radiation Physics and Chemistry, 95 (2014), 420-423.

[6] Mohammad Amir Sattari, Gholam Hossein Roshani, Robert Hanus, Improving the structure of two-phase flow meter using feature extraction and GMDH neural network, Radiation Physics and Chemistry, Volume 171, June 2020, 108725.

[7] S. H. Jung, J. Moon, J. G. Park and J. C. Li , Study on visualization of water mixing flows in a digester equipped with a vertical impeller by using radiotracers. Nuclear Engineering and Technology, 52, 1 (2020), pp.170-177.

[8] E. Abro, V. A. Khoryakov, G. A. Johansen, Determination of Void Fraction and Flow Regime Using a Neural Network Trained on Simulated Data Based on Gamma-Ray Densitometry. Measurement Science and Technology. 10, 7 (1999), 619-630.

[9] T. Cong , R. Chen , G. Su , S. Qiu , W. Tian, Analysis of CHF in saturated forced convective boiling on a heated surface with impinging jets using artificial neural network and genetic algorithm. Nuclear Engineering and Design, 241, 9 (2011). doi:10.1016/j.nucengdes.2011.07.029.

[10] Roshani, G.H. and Nazemi, E., 2017. A high performance gas–liquid two-phase flow meter based on gamma-ray attenuation and scattering. Nuclear Science and Techniques, 28(11), p.169.

[11] Karami, A., Roshani, G.H., Salehizadeh, A. and Nazemi, E., 2017. The fuzzy logic application in volume fractions prediction of the annular three-phase flows. Journal of Nondestructive Evaluation, 36(2), p.35.-500.
[12] T. Cong, G. Su, S. Qiu, W. Tian, Applications of ANNs in flow and heat transfer problems in nuclear engineering: A review work. Progress in Nuclear Energy, 62 (2013), 54-71.
[13] H. Kasban, E. H. Ali and H. Arafa, Diagnosing plant pipeline system performance using radiotracer techniques. Nuclear Engineering and Technology, 49, 1(2017), pp.196-208.
[14] V Mosorov, M Zych, R Hanus, D Sankowski, A Saoud, Improvement of Flow Velocity Measurement Algorithms Based on Correlation Function and Twin Plane Electrical Capacitance Tomography, Sensors 20, 1(2020), 306.
[15] Karami, A., Roshani, G.H., Khazaei, A., Nazemi, E. and Fallahi, M., 2018. Investigation of different sources in order to optimize the nuclear metering system of gas–oil–water annular flows. Neural Computing and Applications, pp.1-13.
[16] J. Krupička, and V. Matoušek, 2014. Gamma-ray-based measurement of concentration distribution in pipe flow of settling slurry: vertical profiles and tomographic maps. Journal of Hydrology and Hydromechanics, 62(2), pp.126-132.
[17] K. Zhang, Y. D. Hou, W. X. Tian, Y. P. Zhang, G. H. Su and S. Z. Qiu, Theoretical prediction of single bubble motion in vertically upward two-phase flow across inclined tube bundles. Annals of Nuclear Energy, 128 (2019), pp.422-432.
[18] V. Roshani, G.H., Nazemi, E. and Roshani, M.M., 2017. Flow regime independent volume fraction estimation in three-phase flows using dual-energy broad beam technique and artificial neural network. Neural Computing and Applications, 28(1), pp.1265-1274.
[19] M. Zych, R. Hanus, B. Wilk, L. Petryka and D. Świsulski, Comparison of noise reduction methods in radiometric correlation measurements of two-phase liquid-gas flows, Measurement, Volume 129 (2018) Pages 288-295.
[20] M. Meribout, M. Meribout, A. Azzi, N. Ghendour, N. Kharoua, L. Khezzar and E. AlHosani, Multiphase Flow Meters Targeting Oil & Gas Industries, Measurement, Volume 165, 1 (2020) 108-111.
[21] D. B. Pelowitz, MCNP-X TM User's Manual, Version 2.5.0. LA-CP-05e0369. Los Alamos National Laboratory (2005).
[22] G.H. Roshani, E. Nazemi, S.A.H. Feghhi, Investigation of using 60Co source and one detector for determining the flow regime and void fraction in gas-liquid two-phase flows, Flow Measurement and Instrumentation, 50 (2016) 73–79.
[23] A. M. Hernandez and J. M. Boone, Tungsten anode spectral model using interpolating cubic splines: unfiltered x-ray spectra from 20 kV to 640 kV. Medical physics, 41, 4 (2014), p.042101.
[24] C. M. Salgado, L. E.B. Brandao, C. M. N. A. Pereira, W. L. Salgado, Salinity independent volume fraction prediction in annular and stratified (water-gas-oil) multiphase flows using artificial neural networks, Progress in Nuclear Energy. 76 (2014) 17-23.
[25] A.G. Ivakhnenko, Polynomial theory of complex systems, IEEE Trans. Syst. Man Cybern. SMC-1, 4 (1971) 364-378.
[26] U. Ozkaya and L. Seyfi, Dimension Optimization of Microstrip Patch Antenna in X/Ku Band via Artificial Neural Network, Procedia - Social and Behavioral Sciences, 195 (2015), 2520-2526.
[27] U. Ozkaya and L. Seyfi, A comparative study on parameters of leaf-shaped patch antenna using hybrid artificial intelligence network models, Neural Computing and Applications, 29 (2018), 35–45.

[28] G. H. Roshani, A. Karami and E. Nazemi, An intelligent integrated approach of Jaya optimization algorithm and neuro-fuzzy network to model the stratified three-phase flow of gas–oil–water. Comp. Appl. Math. 38, 5 (2019). https://doi.org/10.1007/s40314-019-0772-1.
[29] G. H. Roshani, A. Karami, E. Nazemi and F. Shama, Volume fraction determination of the annular three-phase flow of gas-oil-water using adaptive neuro-fuzzy inference system, Comp. Appl. Math. 37(2018), 4321–4341.
[30] G.H. Roshani, A. Karami, A. Khazaei, A. Olfateh, E. Nazemi and M. Omidi, Optimization of radioactive sources to achieve the highest precision in three-phase flow meters using Jaya algorithm, Applied Radiation and Isotopes, 139 (2018), 256–265.
[31] R. Gholipour Peyvandi and S.Z. Islami Rad, Application of artificial neural networks for the prediction of volume fraction using spectra of gamma rays backscattered by three-phase flows, Eur. Phys. J. Plus (2017) 132: 511.
[32] S.Z. Islami rad, R. Gholipour Peyvandi, A simple and inexpensive design for volume fraction prediction in threephase flow meter: Single source-single detector, Flow Measurement and Instrumentation, 69 (2019), 101587.
[33] S. Z. Islami rad, R. Gholipour Peyvandi and S. Sadrzadeh, Determination of the volume fraction in (water-gasoil-air) multiphase flows using a simple and low-cost technique:Artificial neural networks, Physics of Fluids, 31, 9 (2019), 10.1063/1.5109698.